

# UNCERTAINTY ESTIMATION ON GPS TIME TRANSFER

**M. Addouche, F. Meyer, and F. Vernotte**  
**Observatoire de Besançon**  
**41 bis av. de l'observatoire,**  
**25010 Besançon cedex, France**  
**E-mail: addouche@obs-besancon.fr**

## Abstract

*The traditional GPS common view technique, using C/A code receivers, is the main time transfer method used by various timing laboratories over the world. Moreover, this method is used to realize the TAI (Temps Atomique International) and the TA (F) (Temps Atomique Français). Clock offsets between laboratory clocks are determined according to a fixed procedure defined by the CCTF (Comité Consultatif du Temps et des Fréquences). Using this procedure, one can perform on average 54 tracks per day (theoretically 90 tracks per day), providing clock offsets. Each of these clock offsets results from one 780's track and is obtained as a result of a quadratic regression, followed by various model-based corrections and finally a linear regression. The clock offsets are then issued with their standard deviations. However, this simplified estimate does not take into account the statistical properties of the different types of noise present in the measurement. We propose here to rigorously estimate this time uncertainty for various types of noise that characterize the transmitted GPS time offset data. This is achieved by the calculation of the covariance matrix of time samples. This method provides us with the variances of the drift coefficients and of the residuals, in the case of a linear drift model for 1-day sample sets, taking into account the different types of noise. In this paper, we compare the obtained results with simulated and real data over several days.*

## I. GPS TIME TRANSFER

The International Atomic Time (TAI) scale is computed by the Bureau International des Poids et Mesures (BIPM) from a set of atomic clocks distributed in several timing laboratories around the world. The time transfer procedure presently used for the realization of TAI is based on the common view approach [1]. The principle to compare remote clocks for the computation of TAI is to connect each timing laboratory clock to a GPS receiver and to simultaneously observe the same satellite. Thanks to a simultaneous observation of the same satellite by two remote time laboratories, the time offset between each station clock and the satellite clock is deduced by simple subtraction according to the laboratory and satellite positions.

About 50 tracks are realized per day. To compute the TAI, the participating time laboratories have to provide one local-to-GPS time offset value per day. This value is deduced from a linear interpolation of time offset samples accumulated over 1-day tracks (Figure 1). The daily time offset is issued with an estimation uncertainty associated to the interpolation.

## II. TIME DEVIATION DATA INTERPOLATION

The first step when processing the deviation data is to carry out a linear interpolation of the N samples  $\{x_0, x_1, \dots, x_{N-1}\}$  we have gotten every day at the moments  $\{t_0, t_1, \dots, t_{N-1}\}$ . This permits us to estimate the daily time offset and also the uncertainty of this estimate. The method usually used to obtain the interpolated function  $g(t) = at + b$  of this samples is the quadratic least-squares interpolation. The uncertainty is then obtained by estimating the daily standard deviation  $\sigma_D$  as

$$\sigma_D^2 = \frac{1}{N-2} \sum_{i=0}^{N-1} [g(t_i) - x_i]^2 \quad (1)$$

### INTERPOLATION USING CHEBYSHEV POLYNOMIALS

Rather than this method, we use the first two Chebyshev polynomials [2-4] as interpolating functions. The interpolated function  $x(t)$  of the time deviation data is gotten as:

$$x(t) = \rho_0 \phi_0(t) + \rho_1 \phi_1(t) + e(t) \quad (2)$$

where  $\phi_0(t)$ ,  $\phi_1(t)$  are the first and the second Chebyshev polynomial and  $e(t)$  is the error function of the interpolated function  $x(t)$ . This error function assumed random behavior of  $x(t)$ . All the parameters  $\rho_0$  and  $\rho_1$  have the same dimension as  $x(t)$  and are to be estimated by  $\hat{\rho}_0$  and  $\hat{\rho}_1$ . As shown below, this estimate is greatly simplified by orthogonality and normality properties of the Chebyshev interpolating functions.

### ESTIMATION OF THE PARAMETERS

Let us define the vector  $\Phi_j$  associated with the interpolating functions  $\phi_j(t)$  as

$$\Phi_j = \begin{pmatrix} \phi_j(t_0) \\ \vdots \\ \phi_j(t_{N-1}) \end{pmatrix} \quad (3)$$

The matrix  $[\Phi]$  is built as

$$[\Phi] = \begin{pmatrix} \phi_0(t_0) & \phi_1(t_0) \\ \vdots & \vdots \\ \phi_0(t_{N-1}) & \phi_1(t_{N-1}) \end{pmatrix} \quad (4)$$

Let us define now the vector X as

$$X = \begin{pmatrix} x_0 \\ \vdots \\ x_{N-1} \end{pmatrix} \quad (5)$$

According to (2), we may express the vector X as

$$X = [\Phi]P + E \quad (6)$$

where P is the vector of the two parameters we have to estimate, and E the error vector standing for the purely random part of X:

$$P = \begin{pmatrix} \rho_0 \\ \rho_1 \end{pmatrix} \quad \text{and} \quad E = \begin{pmatrix} e(t_0) \\ \vdots \\ e(t_{N-1}) \end{pmatrix} \quad (7)$$

The parameter vector P may be estimated using this formula

$$[\Phi]^T X = [\Phi]^T [\Phi]P + [\Phi]^T E \quad (8)$$

The orthonormality property of the Chebyshev polynomials implies:

$$[\Phi]^T [\Phi] = [I_3] \quad (9)$$

In addition, because of the overall average  $\langle [\Phi]^T E \rangle = 0$  the parameter vector may be estimated as:

$$\hat{P} = [\Phi]^T X \quad (10)$$

Thus, the estimate  $\hat{\rho}_j$  of the parameter  $\rho_j$  is obtained by calculating

$$\hat{\rho}_j = \Phi_j^T \cdot X = \sum_{i=0}^{N-1} \phi_j(t_i) x_i \quad (11)$$

### III. UNCERTAINTY ESTIMATION

The residuals may be defined from (10) as a vector  $\delta$ :

$$\delta = W [\Phi] \hat{P} \quad (12)$$

The variance of the residuals  $\sigma_E^2$  may be estimated by

$$\sigma_E^2 = \frac{1}{N} \langle \delta^T \cdot \delta \rangle \quad (13)$$

Knowing that the overall average  $\langle \delta^T [\Phi] \hat{P} \rangle = 0$  and using (12), we have

$$\langle \delta^T \cdot \delta \rangle = \langle X^T \cdot X \rangle - \langle \hat{P}^T \cdot \hat{P} \rangle \quad (14)$$

One of the main properties of the Chebyshev interpolation parameters is that  $\text{cov}(\rho_0, \rho_1) = 0$  for any type of noise. The variance of the residuals may thus be estimated as

$$\sigma_E^2 = \sigma_X^2 - \frac{1}{N} (\sigma_{\rho_0}^2 + \sigma_{\rho_1}^2) \quad (15)$$

where the variance  $\sigma_X^2$  of the  $x(t)$  is equal to the scalar product  $\frac{1}{N} \langle X^T \cdot X \rangle$ . As for the scalar product  $\langle P^T \cdot P \rangle$ , it is equal to the sum of the variances of each estimate  $\hat{\rho}_0$  and  $\hat{\rho}_1$ .

## ESTIMATION OF THE VARIANCE OF THE RESIDUALS FROM THE NOISE LEVELS

### CORRELATION OF SAMPLES

We have to estimate the uncertainty of time offsets between two time laboratory clocks every day. This estimate must be evaluated according to the level of the various noises that are in the time samples. The autocorrelation function  $R_x(t)$  of these time samples  $x(t)$  contains information about the type and the noise levels. The power spectral density  $S_x(f)$  is the Fourier transform of the autocorrelation function  $R_x(t)$ . The two-sided  $S_x^{2S}(f)$  and the one-sided  $S_x(f)$  power spectral densities are thus defined as

$$\begin{cases} S_x(f) = 2 \cdot S_x^{2S}(f) & \text{if } f \geq 0 \\ S_x(f) = 0 & \text{if } f < 0 \end{cases} \quad (16)$$

so we have

$$\begin{aligned} R_x(t_j - t_i) &= \langle x(t_i) \cdot x(t_j) \rangle \\ &= \int_{-\infty}^{+\infty} S_x^{2S}(f) \cdot e^{+j2\pi f \cdot (t_j - t_i)} \cdot df \\ &= \int_0^{+\infty} S_x(f) \cdot \cos[2\pi f \cdot (t_j - t_i)] \cdot df \end{aligned} \quad (17)$$

By taking into account the low cut-off frequency  $f_l$  and the high cut-off frequency  $f_h$ , we may rewrite (17) as

$$R_x(t_j - t_i) = \int_{f_l}^{f_h} S_x(f) \cdot \cos[2\pi f \cdot (t_j - t_i)] \cdot df \quad (18)$$

We modeled the different types of noise according to the power-law model of  $S_x(f)$  as

$$S_x(f) = \sum_{\alpha=-4}^0 k_\alpha f^\alpha \quad (19)$$

The different types of noise are identified by the values of  $\alpha$  as

- white PM for  $\alpha = 0$ ,
- flicker PM for  $\alpha = -1$ ,
- white FM for  $\alpha = -2$ ,
- flicker FM for  $\alpha = -3$ ,
- random-walk FM for  $\alpha = -4$ .

Table 1 shows the noise levels-based formulas of the autocorrelation function  $R_x(t)$  and also the intercorrelation function  $R_x(t_j - t_i)$  of time offset sequence [4].

Table 1. Correlations of the time offset data  $x(t)$  versus the noise levels  $k_\alpha$ .

$S_x(f)$	$R_x(t_j - t_i)$ (with $i \neq j$ )	$R_x(t)$
$k_{-4}f^{-4}$	$k_{-4}\left[\frac{1}{3f_l^3} - \frac{2\pi^2}{f_l}(t_j - t_i)^2 + \frac{2\pi^4}{3} t_j - t_i \right]$	$\frac{k_{-4}}{3}f_l^3$
$k_{-3}f^{-3}$	$k_{-3}\left[\frac{1}{2f_l^2} + \pi^2(t_j - t_i)^2 \cdot \left(-3 + 2C + 2\ln(2\pi f_l t_j - t_i )\right)\right]$	$\frac{k_{-3}}{2}f_l^2$
$k_{-2}f^{-2}$	$k_{-2}\left[\frac{1}{f_l} - \pi^2 t_j - t_i  + 2Pi^2 f_l(t_j - t_i)^2\right]$	$\frac{k_{-2}}{f_l}$
$k_{-1}f^{-1}$	$k_{-1}\left[-C - \ln(2\pi f_l t_j - t_i ) + \pi^2 f_l^2(t_j - t_i)^2\right]$	$k_{-1} \ln\left(\frac{f_h}{f_l}\right)$
$k_0$	0	$k_0 f_h$

$C \approx 0.5772$  is the Euler constant,  $f_l$  is the low cut-off frequency, and  $f_h$  is the high cut-off frequency.

## VARIANCES OF THE PARAMETERS AND THE RESIDUALS

As shown in (15), we have to calculate the variance of the residuals from the variance of the time offset samples  $x(t)$  and that of the parameters  $\hat{\rho}_0$  and  $\hat{\rho}_1$ . Thus, we have to know  $\sigma_x^2$  and the  $\sigma_{\rho_i}^2$ .

The variance of  $x(t)$  is given as

$$\sigma_x^2 = \langle x^2(t) \rangle = R_x(t) \quad (20)$$

Let us consider the covariance matrix of the parameters as

$$[C_v] = \langle \hat{P} \cdot \hat{P}^T \rangle = [\Phi]^T \langle X \cdot X^T \rangle [\Phi] \quad (21)$$

Considering the element whose position in the matrix is (i, j), we may write

$$\langle X \cdot X^T \rangle \Big|_{i,j} = R_x(t_j - t_i) \quad (22)$$

thus

$$[C_v]_{i,j} = \sum_{k=0}^{N-1} \phi_j(t_k) \cdot \sum_{l=0}^{N-1} R_x(t_l - t_k) \cdot \phi_i(t_l) \quad (23)$$

then

$$\langle \hat{P}_i \cdot \hat{P}_j \rangle = [C_v]_{i,j} = \sum_{k=0}^{N-1} \sum_{l=0}^{N-1} R_x(t_l - t_k) \cdot \phi_i(t_l) \cdot \phi_j(t_k) \quad (24)$$

and so

$$\sigma_{\rho_i}^2 = \langle \hat{P}_i^2 \rangle = [C_v]_{i,i} \quad (25)$$

Finally, the variance of the residuals is thus calculated according to (15) with the values of the variance of the time offset samples given by (20) and also with the variances of the interpolating parameters (Table 2) shown in (25). This uncertainty estimation of the interpolated time offset value is realized using only the noise levels, since it is based on the autocorrelation function of the time offset samples.

Table 2. Variance of the interpolation parameters  $\sigma_{\rho_0}^2$  and  $\sigma_{\rho_1}^2$  versus the noise levels  $k_\alpha$  [4].

$S_x(f)$	$\sigma_{\rho_0}^2$	$\sigma_{\rho_1}^2$
$k_{-4} f^{-4}$	$\frac{4 N k_{-4}}{3 f_l^3}$	$\frac{\pi^2 N^3 \tau_0^2 k_{-4}}{3 f_l}$
$k_{-3} f^{-3}$	$\frac{3 N k_{-3}}{2 f_l^2}$	$\left[7 - 4 \ln(2\pi N \tau_0 f_l) - 4C\right] \frac{\pi^2 N^3 \tau_0^2 k_{-3}}{12}$
$k_{-2} f^{-2}$	$\frac{2 N k_{-1}}{f_l}$	$\frac{\pi^2 N^2 \tau_0 k_{-2}}{5}$
$k_{-1} f^{-1}$	$\left[3 - 2 \ln(2\pi N \tau_0 f_l)\right] \frac{N k_{-1}}{2}$	$\frac{3 N k_{-1}}{4}$
$k_0$	$k_0 f_h$	$k_0 f_h$

The coefficients  $\{k_0, \dots, k_4\}$  represent the noise levels of the power spectral density of the time offset.  $C \approx 0.5772$  is the Euler constant.  $\tau_0$  is the time offset sampling period. The low cut-off frequency  $f_l$  is assumed to be much lower than  $\frac{1}{N\tau_0}$ . Assuming a sampling satisfying the Shannon rule, the high cut-off frequency is  $f_h = \frac{1}{2\tau_0}$ .

## EXPERIMENTAL VALIDATION

### COHERENCE ASSESSMENT USING SIMULATION

Aiming at realizing the assessment of the uncertainty estimation given by (15), (20) and (25), we first identified the different noise types the time offset samples actually contains. Then we generated a set of sampled signals in accordance with the levels of these noise types.

Figure 2 shows a real data sequence taken as an example to be analyzed. It represents time connection data between the *Observatoire de Besançon* and the *Observatoire de Paris* between 7 September 2003 and 2 December 2003. From this signal, we generated 1000 time deviation sequences of 26 days. We determined the levels of the different types of noise as in [3,6]. According to the obtained results, only white FM and white PM with the levels found are included in the

simulated sequences.

To compare the classical uncertainty estimation  $\sigma_D$  as in (1) and the noise-based uncertainty  $\sigma_E$  given by (15), we reflected the value of the noise-based standard deviation we calculate over 26 days on all of the set of daily standard deviations. As shown in Figure 3, the new uncertainty estimation  $\sigma_E^2$  we calculated over a fixed number of days agrees with the daily uncertainty values  $\sigma_D^2$ .

Figure 4 represents the dispersion of the noise-based standard deviation  $\sigma_E$  and that of the daily standard deviation  $\sigma_D$ . This result is obtained from the 1000 sequences we generated. These standard deviations show a  $\chi^2$  law. However, the dispersion of the noise-based variance is about 5 times thinner than the dispersion of the statistic-based one. We may thus conclude that the noise-based uncertainty estimation is a better indicator than the daily uncertainty.

Taking into consideration the  $\chi^2$  distribution of the uncertainty dispersion, we rate the value interval where the daily standard deviations should be included. For example, in Figure 4  $\sigma_E = 2.68 \text{ ns}$  and the number of degrees of freedom  $l = 90$ . The confidence interval of 90% is determined [5] to be

$$0.812 \cdot \sigma_E^2 < \sigma_D^2 < 1.336 \cdot \sigma_E^2 \quad (26)$$

According to the value of  $\sigma_E$ , we calculate the confidence interval of 90% to be estimated as

$$2.411 < \sigma_D < 3.093 \quad (27)$$

The result is represented in Figure 5 in the case of one example among the 1000 sequences we simulated. It shows again the good agreement between the daily uncertainty estimation and the noise-based one via the deduced confidence interval.

## REAL TIME TRANSFER DATA

We operated the noise-based uncertainty estimation on the real data we used above to determine the typical noise levels. The results are shown in Figure 6. We notice that the time transfer uncertainty based on the noise-based variance  $\sigma_E^2$  is relatively underestimated compared to the daily uncertainty that is calculated as in (1). The difference is evaluated on average to be 15%.

Several differences between the simulated data and the real time offset samples may explain this difference: On the one hand, some samples are actually missing sporadically, while the simulated signals are always complete. On the other hand, there are some occasional high dispersions of time offset evaluation. These may explain why the estimation of the daily standard deviation  $\sigma_D$  has been overestimated.

## IV. CONCLUSIONS

On GPS time transfer, the quadratic least-squares interpolation is the usual method to estimate the daily time offset between two time laboratory clocks. This time offset information is issued with other significant information, namely the time offset uncertainty. That information is obtained by the calculation of the daily standard deviation of the residuals of the interpolated samples.

In this work, we chose to perform Chebyshev interpolation in order to lead to a formulation of the time transfer uncertainty according to noise levels contained in the GPS time offset data. We saw that the results show a good agreement with the simulated time offset signals. They also proved that the

noise-based uncertainty estimation over a few days is a better indicator than the daily uncertainty estimation. However, we noticed that in the case of real time offset samples, the uncertainty was underestimated compared to the set of daily standard deviations. This discrepancy is probably due, on the one hand, to a few sporadically missing samples which are not taken into account in the simulations. On the other hand, the connection discontinuity and perhaps also the occasional dispersion imply an increase in the daily standard deviation when the noise-based one is estimated in accordance of the noise levels over several days.

As the noise-based estimation agreement with the classical one is checked in this work, that discrepancy does not question the truthfulness of the noise-based uncertainty we formulated. But it shows the necessity to evaluate the inherent uncertainty offset due to the occasional dispersion and discontinuity and also the necessity to take into account missing samples.

## GLOSSARY OF SYMBOLS

---

$\sigma_D$	Standard deviation of the residuals estimated statistically over 1 day
$N$	Number of samples in a 1-day track
$g(t)$	Linear interpolation function of the time offset samples $x_i$
$x_i$	time offset samples at the moments $t_i$
$a, b$	Linear interpolation parameters of $g(t)$
$t_i$	Sampling moments
$x(t)$	Time offset sample: the time difference between the remote and local clocks
$\phi_i(t)$	with $i \in \{0,1\}$ . The 1 <sup>st</sup> and 2 <sup>nd</sup> Chebyshev polynomials. $i$ is the degree of the polynomial
$\rho_i$	with $i \in \{0,1\}$ . The first and second Chebyshev parameters
$e(t)$	Purely random behavior of the time offset $x(t)$
$\hat{\rho}_i$	with $i \in \{0,1\}$ . Estimates of the first and second Chebyshev parameters
$\Phi_i$	Vector whose $N$ components are the values of $\phi_i(t)$ at each measurement time
$[\Phi]$	Matrix of two column vectors $\Phi_0$ and $\Phi_1$
$P$	Vector whose components are the first and the second Chebyshev parameters
$E$	Vector form of $e(t)$ . The components of $E$ are the values of $e(t)$ for each sample $x_i$
$X$	Vector form of $x(t)$ . The components of $X$ are the $N$ time offset samples
$[I_m]$	The unit matrix $m \times m$
$\hat{P}$	Vector whose components are the estimates of the 1 <sup>st</sup> and 2 <sup>nd</sup> Chebyshev parameters
$\delta$	Vector whose components are the $N$ residuals of the interpolated sequence
$\sigma_E$	Standard deviation of the residuals estimates in accordance with the noise levels
$\sigma_X$	Standard deviation of the time offset sample $x(t)$
$\sigma_{\rho_i}$	Standard deviation of the Chebyshev parameters $\rho_i$
$S_x(f)$	One-sided power spectral density of the time offset sequence $x(t)$
$S_x^{2S}(f)$	Two-sided power spectral density of the time offset sequence $x(t)$
$R_x(t)$	Autocorrelation function of the time offset sequence $x(t)$
$f_l$	Low cut-off frequency of the spectral density $S_x(f)$
$f_h$	High cut-off frequency of the spectral density $S_x(f)$
$k_\alpha$	Noise level associated with the $f^\alpha$ noise of the power spectral density of time offset $S_x(f)$
$[C_v]$	Covariance matrix of the Chebyshev parameters $\rho_0$ and $\rho_1$

---

## REFERENCES

- [1] D. W. Allan and M. Weiss, 1980, “Accurate time and frequency transfer during common-view of a GPS satellite,” in Proceedings of the 34<sup>th</sup> Annual IEEE Frequency Control Symposium, 28-30 May 1980, Philadelphia, Pennsylvania, USA (NTIS AD-A213670), pp. 334-356.
- [2] J. E. Deeter and P. E. Boynton, 1982, “Techniques for the estimation of red power spectra. I. Context and methodology,” **Astrophysical Journal**, **261**, 337-350.
- [3] F. Vernotte, 1999, “Estimation of the power spectral density of phase: comparison of three methods,” in Proceedings of the Joint Meeting of the 13<sup>th</sup> European Frequency and Time Forum (EFTF) and the IEEE International Frequency Control Symposium, 13-16 April 1999, Besançon, France (IEEE Publication 99CH36313), pp. 1109-1112.
- [4] F. Vernotte, J. Delporte, M. Brunet, and T. Tournier, 2001, “Uncertainty of drift coefficients and extrapolation errors: application to clock error prediction,” **Metrologia**, **38**, 325-342.
- [5] G. Saporta, 1990, **Probabilités, analyse des données et statistique** (Editions Technip, Paris), ISBN 2-7108-0565-0.
- [6] F. Vernotte, E. Lantz, J. Groslambert, and J. J. Gagnepain, 1993, “Oscillator noise analysis: multivariance measurement,” **IEEE Transactions on Instrumentation and Measurement**, **IM-42**, 342-350.

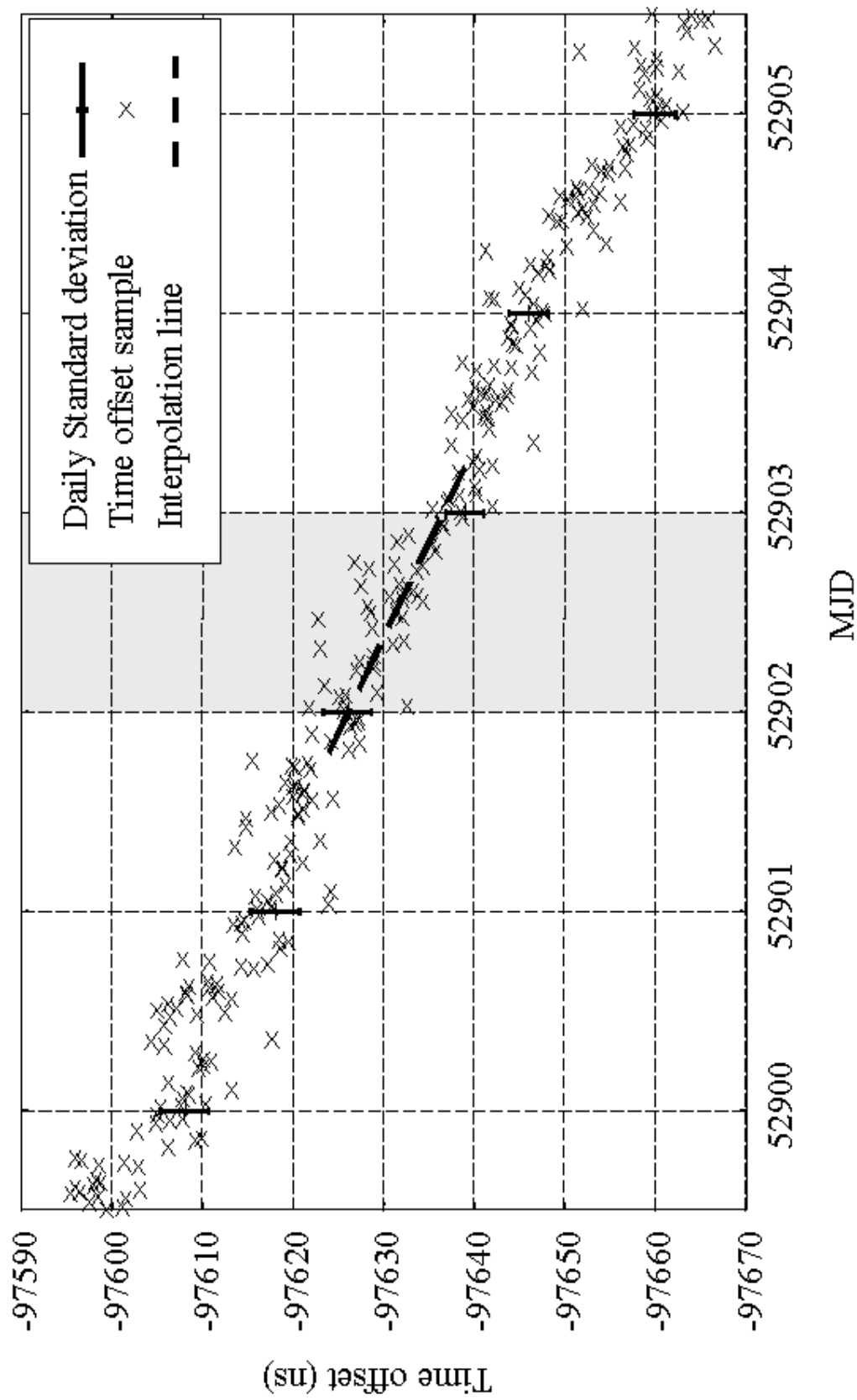


**Figure 1.** Time offset signal between two time laboratory clocks. Dashed line represents the daily interpolation line usually performed to estimate the daily time offset issued with the daily standard deviation.

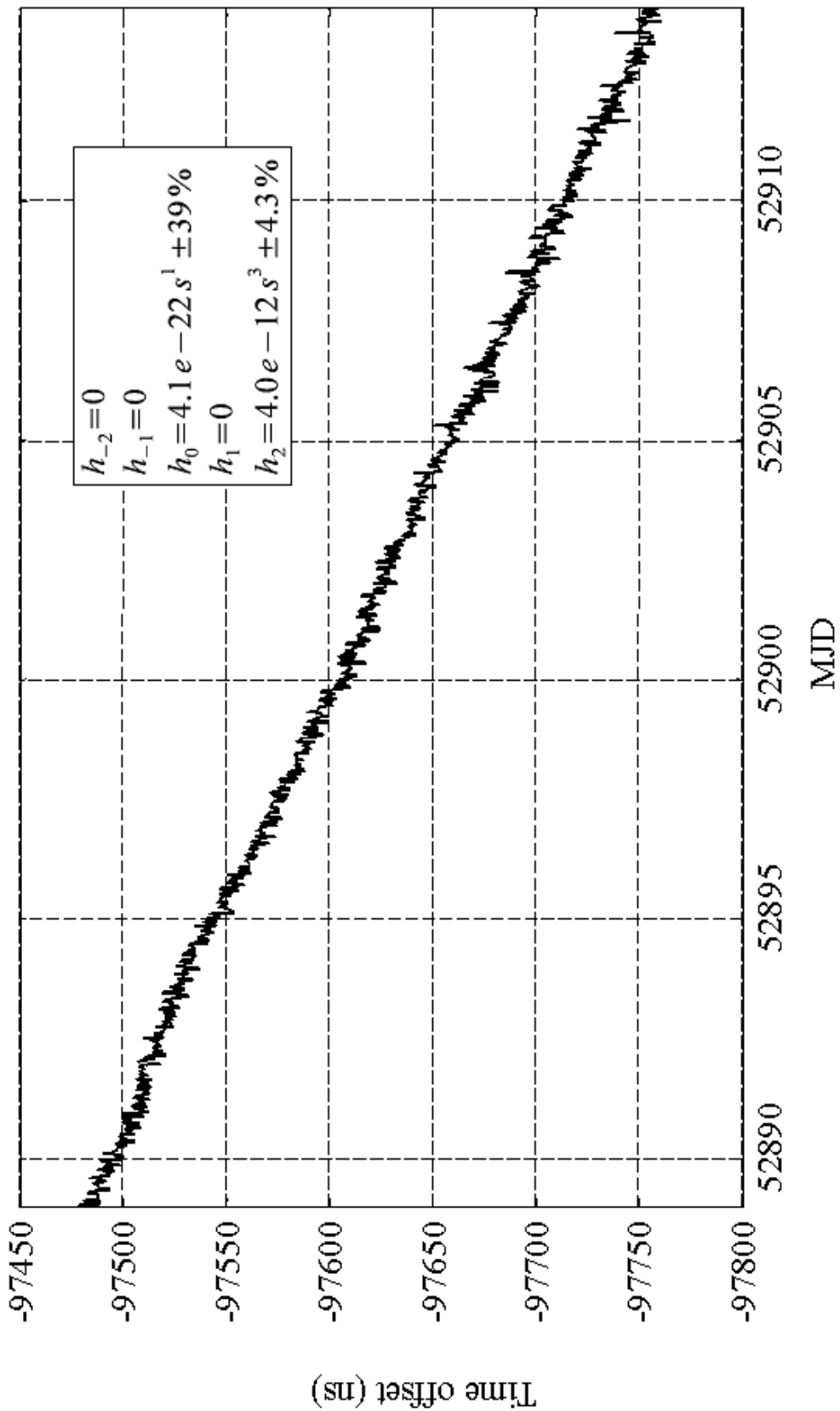


**Figure 2.** Real time offset samples between the *Laboratoire de Besançon* and the *Laboratoire de Paris* (September seventh 2003 to December second 2003). This signal is used as a model to generate about one thousand simulated time offset sequences. They have the same noise levels as this real signal.

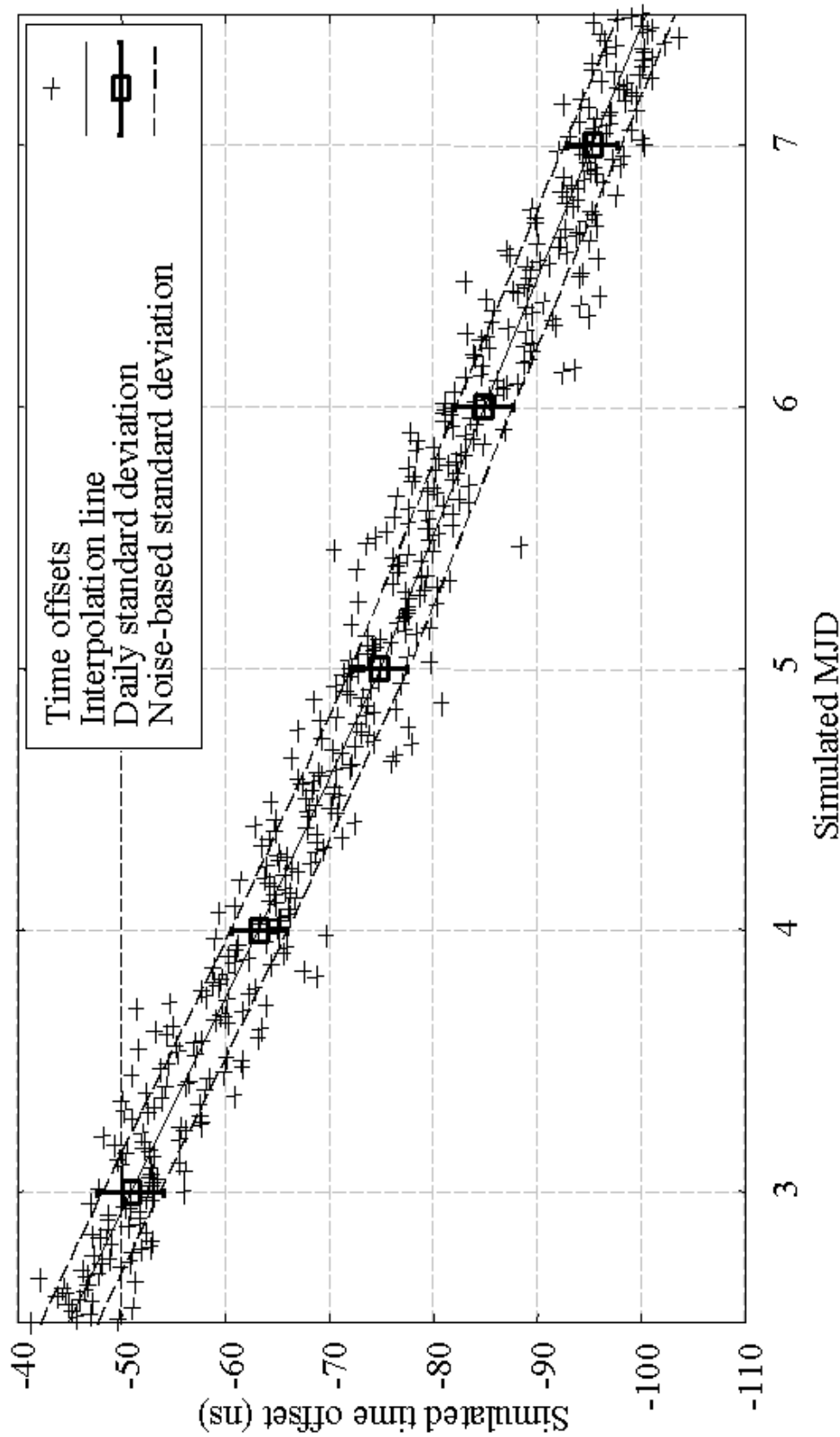


**Figure 3.** Assessment of the noise-based estimation of time transfer uncertainty for a simulated sequence. Cross (+) represent simulated time offsets (e.g. over 5 days). The boxes with its error bar represent the daily interpolated time offset and its standard deviation. Dashed lines represent the noise-based standard deviation on around the interpolation solid line.

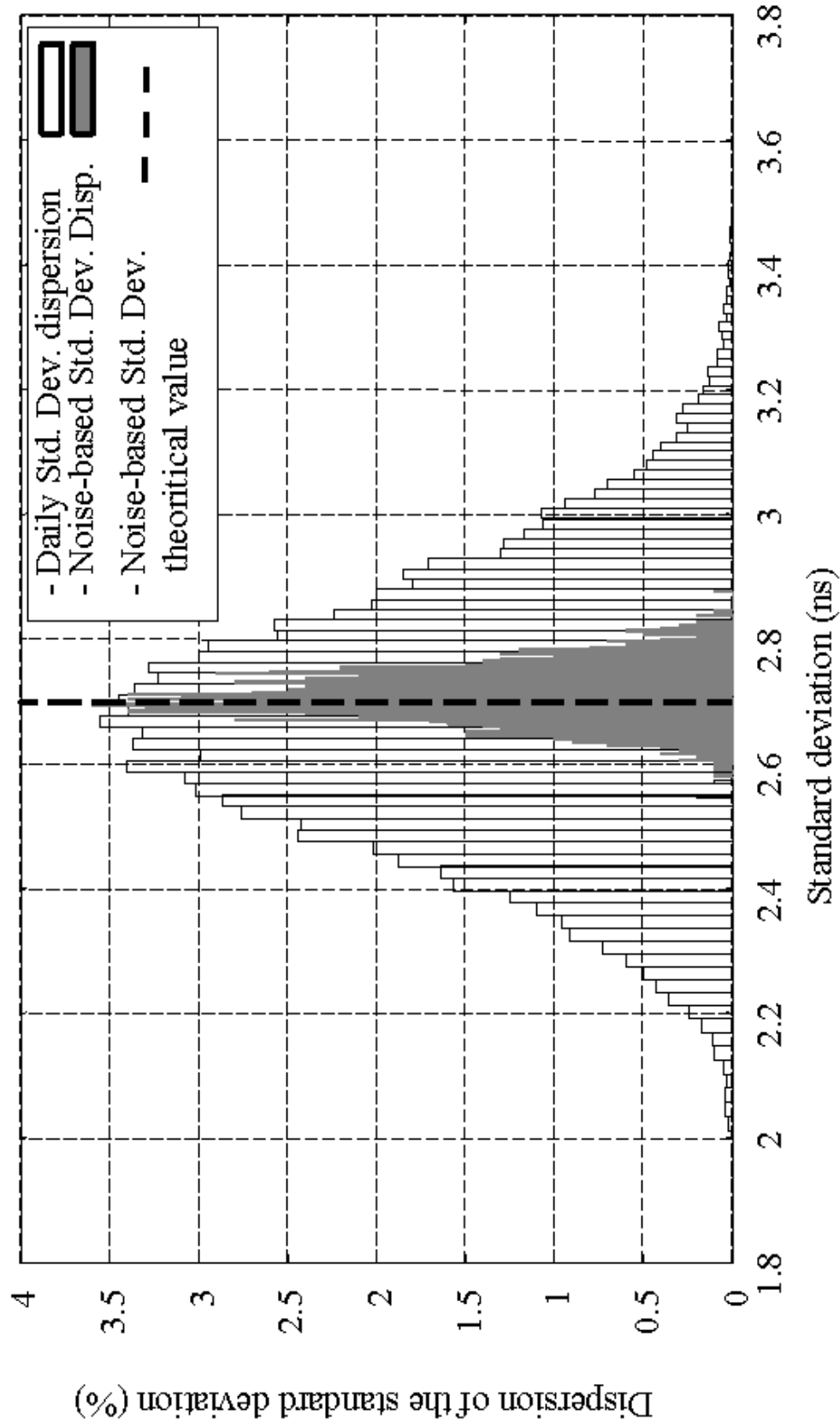


**Figure 4.** Dispersion for one thousand sequences of the noise-based standard deviation (in bold gray boxes) and the daily standard deviation (in hollow boxes). Dashed line represents the theoretical noise-based standard deviation according to the noise levels entered for the simulation.

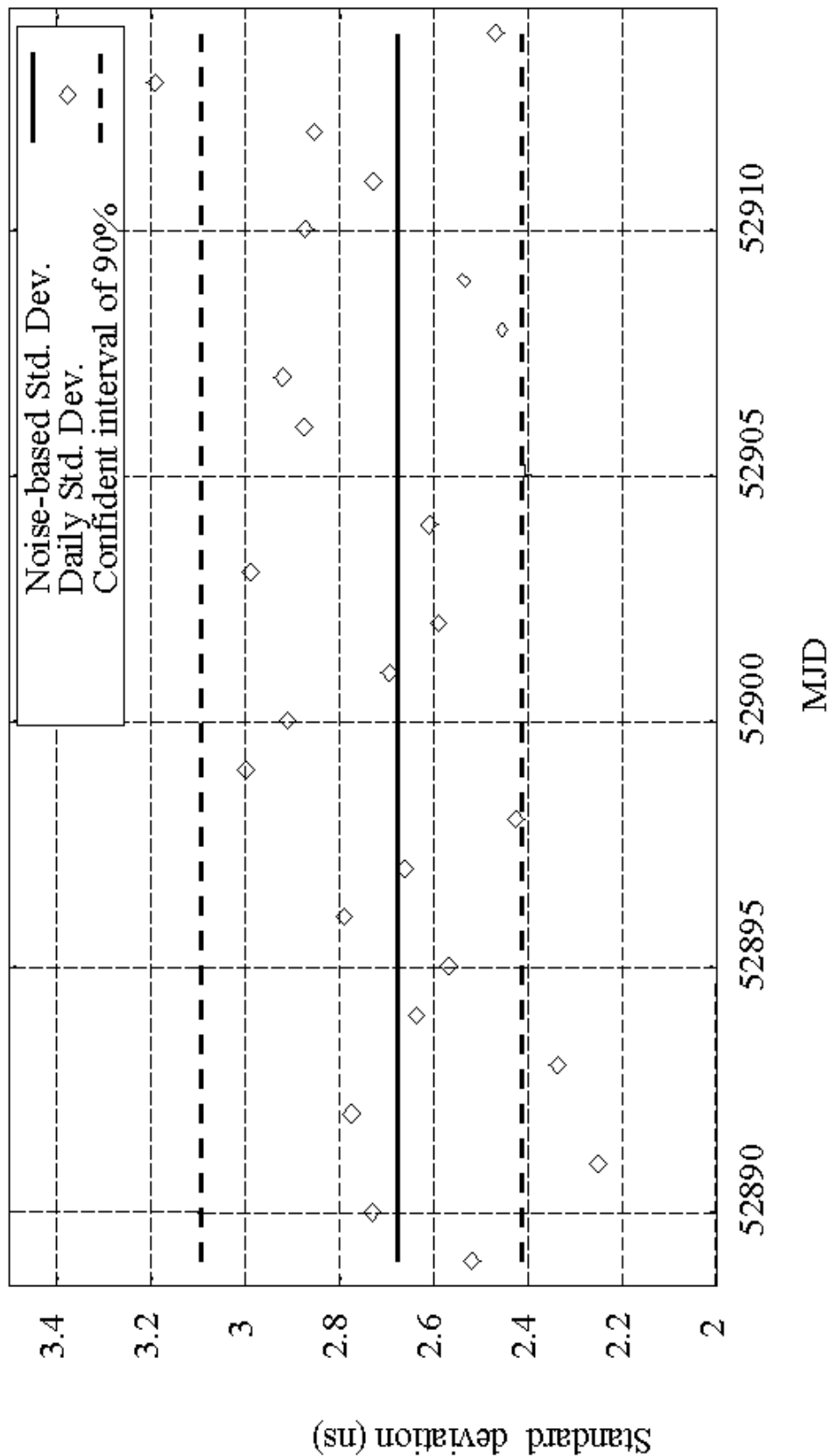


**Figure 5.** Distribution of daily standard deviations. Rhombuses represent the daily standard deviation over about 26 days. Solid line represents the value of the noise-based standard deviation. Dashed lines represent bottom and top limits of the noise-based standard deviation interval according to the student table [5] (confidence interval of 90% in case of a  $\chi^2$  law of a fixed number of degrees of freedom.)

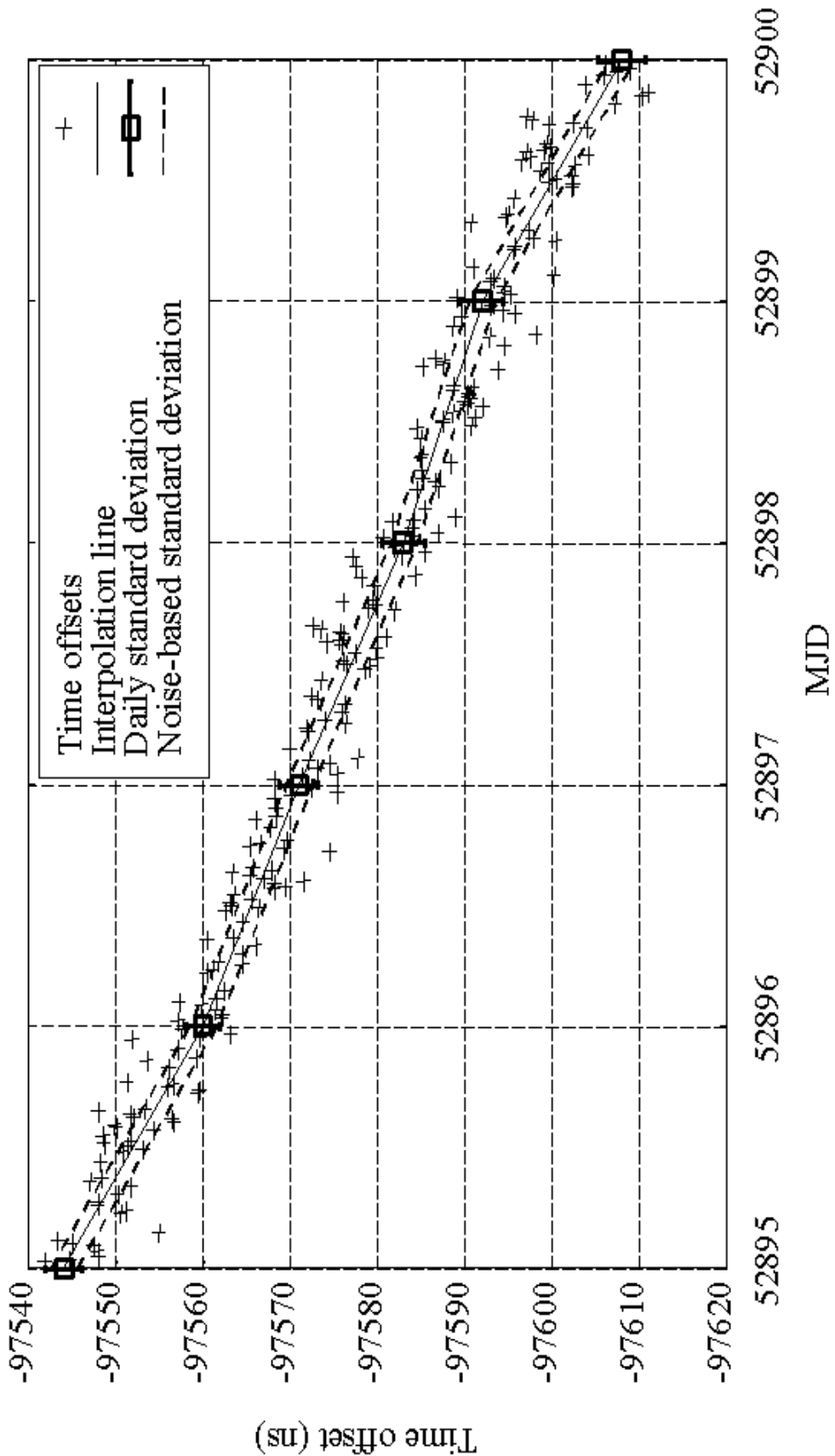


**Figure 6.** Assessment of the noise-based estimation of time transfer uncertainty for a real data sequence. Cross (+) represent simulated time offsets (eg. over 5 days). The boxes and its error bar represent the daily interpolated time offset and its standard deviation. Dashed lines represent the noise-based standard deviation on around the interpolation solid line

## **QUESTIONS AND ANSWERS**

**JOHN DAVIS (National Physical Laboratory, UK):** Did you do any statistics just looking at GPS measurements at the single epoch? That is, measurements that were all taken at the same time, presuming that you were using a multi-channel GPS receiver? Are you using a multi-channel GPS receiver to make your measurements?

**MAHMOUD ADDOUCHÉ:** I use the BIPM schedule. So I track one satellite at one time.

**DAVIS:** The point was that if you are using a multi-channel receiver and you are making your measurements at the same epoch, then if you look at the statistics on that, you will be independent of the clock noise; whereas, if you are making measurements at successive epochs with a single-channel receiver, you are going to get a mixture of clock and time transfer noise. This is an easy way of distinguishing the two, which might help you.

**ADDOUCHE:** It will be interesting, but I didn't see this.

**DAVIS:** There should be plenty of data available for you to have a look at. We can provide you with that.

